GEOPHYSICS, VOL. 75, NO. 3 (MAY-JUNE 2010); P. O21–O37, 17 FIGS., 3 TABLES.
10.1190/1.3386676

Probabilistic petrophysical-properties estimation integrating statistical rock physics with seismic inversion

Dario Grana[1] and Ernesto Della Rossa[1]

ABSTRACT

A joint estimation of petrophysical properties is proposed that combines statistical rock physics and Bayesian seismic inversion. Because elastic attributes are correlated with petrophysical variables (effective porosity, clay content, and water saturation) and this physical link is associated with uncertainties, the petrophysical-properties estimation from seismic data can be seen as a Bayesian inversion problem. The purpose of this work was to develop a strategy for estimating the probability distributions of petrophysical parameters and litho-fluid classes from seismics. Estimation of reservoir properties and the associated uncertainty was performed in three steps: linearized seismic inversion to estimate the probabilities of elastic parameters, probabilistic upscaling to include the scale-changes effect, and petrophysical inversion to estimate the probabilities of petrophysical variables and litho-fluid classes. Rock-physics equations provide the linkbetween reservoir properties and velocities, and linearized seismic modeling connects velocities and density to seismic amplitude. A full Bayesian approach was adopted to propagate uncertainty from seismics to petrophysics in an integrated framework that takes into account different sources of uncertainty: heterogeneity of the real data, approximation of physical models, measurement errors, and scale changes. The method has been tested, as a feasibility step, on real well data and synthetic seismic data to show reliable propagation of the uncertainty through the three different steps and to compare two statistical approaches: parametric and nonparametric. Application to a real reservoir study (including data from two wells and partially stacked seismic volumes) has provided as a main result the probability densities of petrophysical properties and litho-fluid classes. It demonstrated the applicability of the proposed inversion method.

INTRODUCTION

In reservoir characterization studies constrained by seismic data, statistical rock physics normally is used to combine statistical techniques with physical equations to generate different petroelastic scenarios. The goal of statistical rock physics is to predict the probability of petrophysical variables when velocities (or impedances) and density are assigned, and to capture the heterogeneity and complexity of the rocks and the uncertainty associated with theoretical relations.

The use of statistics in rock physics is becoming more frequent. In the typical statistical rock-physics workflow (Avseth et al., 2005; Doyen, 2007), deterministic models first are established to build physical relations between elastic properties and reservoir attributes. Then, probabilistic petroelastic transformations are determined, combining these relations with Monte Carlo simulations, to include the uncertainty associated with the real data (measurement errors and natural heterogeneity of the rocks) and with the degree of accuracy of the model itself.

The traditional Bayesian framework (Tarantola, 2005) used for uncertainty evaluation in elastic inversion (Buland and Omre, 2003) has been adopted recently for problems of litho-fluid prediction from seismic data (Larsen et al., 2006; Gunning and Glinsky, 2007; and Buland et al., 2008).

Mukerji et al. (2001) and Eidsvik et al. (2004) introduce statistical rock physics to estimate reservoir parameters from prestack seismic data and to evaluate the associated uncertainty. Stochastic rock-physics models are used by Bachrach (2006) for a joint estimation of porosity and saturation and by Sengupta and Bachrach (2007) for pay-volume uncertainty evaluation, and Spikes et al. (2008) develop a probabilistic seismic inversion to constrain reservoir properties estimation with well data and seismic. To infer litho-fluid classification from seismic data, Larsen et al. (2006) propose an integrated litho-fluid-inversion method based on a Markov-chain model, and Gallop

Manuscript received by the Editor 8 May 2009; revised manuscript received 9 November 2009; published online 26 May 2010; corrected version published online 27 May 2010.
[1]Eni Exploration and Production, San Donato Milanese, Italy. E-mail: dario.grana@eni.it; ernesto.dellarossa@eni.it

(2006) presents an approach based on mixture distributions for facies estimations. González et al. (2008), and Bosch et al. (2009) propose new approaches integrating advanced geostatistical techniques.

In this paper, we present a method to integrate statistical rock physics and Bayesian elastic inversion to compute the probability distributions of petrophysical properties. Similar approaches already have been presented, with some assumptions and limitations about the form of the probability distributions, the size of the data, and the type of dependencies considered. By means of more general parametric distributions, such as Gaussian mixture models (GMMs) (Hastie et al., 2002), or nonparametric statistical techniques like kernel density estimation (KDE) (Silverman, 1986), some limitations can be overcome by our approach. We also take into account the upscaling problem (Lake and Srinivasan, 2004) to face the limited resolution and greater uncertainty of seismic data compared to well-log data and we integrate this step within the probabilistic inversion framework.

The workflow we propose (Figure 1) can be summarized as follows:

1) Rock-physics model calibration. A rock-physics model is established using well-log data to predict elastic attributes (velocities or impedances) from petrophysical properties.
2) Linearized Bayesian seismic inversion. We estimate elastic properties from partially stacked seismic angle gathers.
3) Conditional probabilities estimation. We calculate the conditional probabilities of petrophysical variables and litho-fluid classes in a multiproperty, multiscale model. This method includes the upscaling effect within an integrated probabilistic approach.

The rock-physics model is a set of equations that transforms petrophysical variables in elastic attributes. The rock-physics model type depends on the reservoir rocks we are dealing with: the set of equations can be a simple regression on well data or a more complex physical model (Mavko et al., 2003). Once the rock-physics model has been calibrated on well logs, we can apply the model to situations not sampled by log data and generate different scenarios by means of Monte Carlo simulations. This approach is used to explore, for example, all possible ranges of porosity, saturation, and clay content, and to simulate the corresponding acoustic and elastic responses.

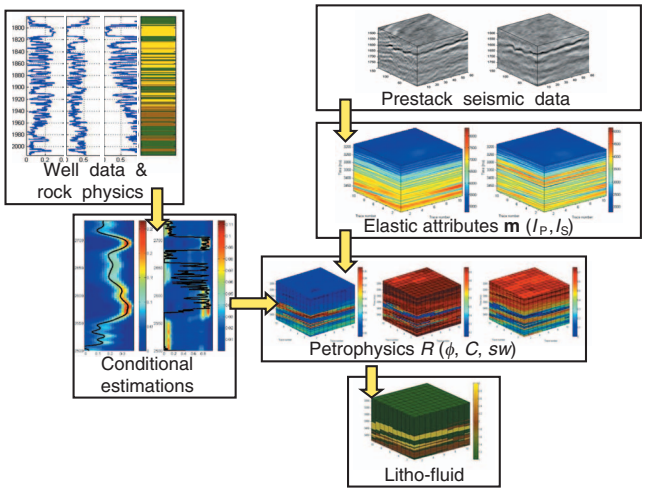

Figure 1. Flowchart of the probabilistic petrophysical-properties estimation

Our proposed method propagates the uncertainty from seismic data to petrophysics by combining three conditional probabilities. The first is the probability of elastic properties given seismic data obtained by a Bayesian approach to elastic inversion (Buland and Omre, 2003). The second is the probability of elastic attributes at fine scale (high resolution) when coarse-scale values are known. The third is the probability of petrophysical properties conditioned by elastic attributes obtained by integrating the rock-physics model equations with Monte Carlo simulations and generating different geologic scenarios.

We applied the method to a clastic reservoir in the North Sea, where two wells and four partially stacked seismic angle gathers are available. As a feasibility step, we tested the method on a calibration well using a synthetic seismic trace and compared two approaches: GMMs and KDE. Then we applied the method to the whole seismic volume and obtained, trace-by-trace, the probability density functions of petrophysical variables and litho-fluid classes.

PROBABILISTIC APPROACH TO PETROPHYSICAL INVERSION

In this section, we illustrate the probabilistic formulation of the joint petrophysical inversion. We describe the derivation of posterior probabilities of petrophysical properties and litho-fluid classes, conditioned by seismics, using different attributes (elastic, petrophysical, and categorical) and integrating data coming from different sources (high-resolution well data, coarse-resolution data, and seismic data).

The methodology is divided in three steps: (1) statistical rock-physics modeling, (2) upscaling, and (3) petrophysical inversion from seismic data.

In the following, we will use $\mathbf{m}$ to indicate the acoustic and elastic properties, typically impedances I_P and I_S ($\mathbf{m} = [I_P\ I_S]^T$), and $\mathbf{R}$ to represent petrophysical data, typically effective porosity, water saturation, and clay content ($\mathbf{R} = [\phi\ sw\ C]^T$).

Statistical rock-physics modeling

One important aspect of statistical rock-physics is that it combines physical models with statistics to account for situations not seen in the well data. If all variables are considered as random vectors, the rock-physics model can be written as

$$\mathbf{m} = \mathbf{f}_{\mathrm{RPM}}(\mathbf{R}) + \boldsymbol{\varepsilon}, \tag{1}$$

where $\mathbf{f}_{\mathrm{RPM}}$ represents the rock-physics model and $\boldsymbol{\varepsilon}$ is the random error describing the degree of accuracy of the model.

For the prior distribution, which is the same at any depth, we assume a multivariate Gaussian mixture (GM), a linear combination of Gaussian distributions, with a fixed number of components N_c:

$$P(\mathbf{R}) = \sum_{k=1}^{N_c} \alpha_k N(\mathbf{R}; \boldsymbol{\mu}_{\mathbf{R}}^k, \boldsymbol{\Sigma}_{\mathbf{R}}^k), \tag{2}$$

where N indicates the multi-Gaussian distribution of vector $\mathbf{R}$ with mean $\boldsymbol{\mu}_{\mathbf{R}}^k$ and covariance matrix $\boldsymbol{\Sigma}_{\mathbf{R}}^k$ for all $k = 1,\ldots,N_c$ and α_k are the weights of the linear combination (with $\sum_{k=1}^{N_c} \alpha_k = 1$).

This choice is motivated by two reasons. First, this formulation allows us to model each litho-fluid class detectable from a petrophysical point of view as a single Gaussian component of the mixture. Second, the approach is convenient analytically because the analytical results valid for Gaussian distributions also can be extended to Gaussian mixtures. We use three components initially in our tests because the litho-fluid classification we consider consists of shale, oil sand, and water sand.

We propose a semianalytical approach for estimation of the conditional probability $P(\mathbf{R}|\mathbf{m})$: we generate a set of N_s samples from the prior distribution $P(\mathbf{R})$, apply the rock-physics model $\mathbf{f}_{\text{RPM}}$, estimate the joint distribution assuming a Gaussian mixture distribution, and analytically derive the conditional distribution.

From the prior distribution, different scenarios can be generated by Monte Carlo simulation. Petrophysical variables can be sampled from the prior distribution and the elastic response can be computed by the rock-physics model $\mathbf{f}_{\text{RPM}}$. We model the vertical correlation of petrophysical properties by means of a vertical variogram to obtain pseudologs of elastic variables with a realistic vertical correlation and subsequently perform upscaling on elastic variables in the probabilistic upscaling step.

We made the additional assumption that error $\boldsymbol{\varepsilon}$ in equation 1 is Gaussian with zero mean and covariance $\boldsymbol{\Sigma}_{\boldsymbol{\varepsilon}}$ that can be estimated from well-log data. With this assumption, we can state that

$$P(\mathbf{m}|\mathbf{R}) = N(\mathbf{m};\boldsymbol{\mu}(\mathbf{R}),\boldsymbol{\Sigma}_{\boldsymbol{\varepsilon}}), \tag{3}$$

where the mean $\boldsymbol{\mu}(\mathbf{R}) = \mathbf{f}_{\text{RPM}}(\mathbf{R})$ and covariance matrix $\boldsymbol{\Sigma}_{\boldsymbol{\varepsilon}}$ can be assumed independent of $\mathbf{R}$ and related only to $\boldsymbol{\varepsilon}$.

This model allows us to account for uncertainty associated with rock-physics model predictions by means of Monte Carlo simulations and conditional probabilities estimations. In fact, we can generate a set of N_s samples $\{\mathbf{R}_i\}_{i=1,\ldots,N_s}$ from the petrophysical prior $P(\mathbf{R})$; then we compute the response of the rock-physics model $\boldsymbol{\mu}(\mathbf{R}_i) = \mathbf{f}_{\text{RPM}}(\mathbf{R}_i)$, for all $i = 1,\ldots,N_s$ and generate N_s samples $\{\mathbf{m}_i\}_{i=1,\ldots,N_s}$ from the normal distributions $N(\mathbf{m};\boldsymbol{\mu}(\mathbf{R}_i),\boldsymbol{\Sigma}_{\boldsymbol{\varepsilon}})$.

Joint distribution $P(\mathbf{m},\mathbf{R})$ can be estimated from the N_s samples $\{(\mathbf{m}_i,\mathbf{R}_i)\}_{i=1,\ldots,N_s}$. If the joint distribution is a Gaussian mixture

$$P(\mathbf{m},\mathbf{R}) = \sum_{k=1}^{N_c} \pi_k N([\mathbf{m},\mathbf{R}]^T;\boldsymbol{\mu}^k_{[\mathbf{m},\mathbf{R}]},\boldsymbol{\Sigma}^k_{[\mathbf{m},\mathbf{R}]}), \tag{4}$$

then conditional distribution $P(\mathbf{R}|\mathbf{m})$ is again a Gaussian mixture. If the rock-physics model $\mathbf{f}_{\text{RPM}}$ were linear, the joint distribution could be derived analytically from the prior, but in general, $\mathbf{f}_{\text{RPM}}$ is not linear and joint distribution $P(\mathbf{m},\mathbf{R})$ can be obtained from the Monte Carlo samples. The technique adopted to estimate parameters of the Gaussian components and weights of the mixture is the expectation-maximization (EM) algorithm (Hastie et al., 2002). We point out that these weights can be interpreted as the indicator probability of the discrete random variable that represents the litho-fluid class.

As a consequence, the conditional distribution $P(\mathbf{R}|\mathbf{m})$ is a Gaussian mixture,

$$P(\mathbf{R}|\mathbf{m}) = \sum_{k=1}^{N_c} \lambda_k N(\mathbf{m};\boldsymbol{\mu}^k_{\mathbf{R}|\mathbf{m}},\boldsymbol{\Sigma}^k_{\mathbf{R}|\mathbf{m}}), \tag{5}$$

and we can analytically compute its parameters. In particular, the means and covariance matrices of the mixture components (see Appendix A) are given by

$$\boldsymbol{\mu}^k_{\mathbf{R}|\mathbf{m}} = \boldsymbol{\mu}^k_{\mathbf{R}} + \boldsymbol{\Sigma}^k_{\mathbf{R},\mathbf{m}}(\boldsymbol{\Sigma}^k_{\mathbf{m},\mathbf{m}})^{-1}(\mathbf{m} - \boldsymbol{\mu}^k_{\mathbf{m}}) \tag{6}$$

and

$$\boldsymbol{\Sigma}^k_{\mathbf{R}|\mathbf{m}} = \boldsymbol{\Sigma}^k_{\mathbf{R},\mathbf{R}} - \boldsymbol{\Sigma}^k_{\mathbf{R},\mathbf{m}}(\boldsymbol{\Sigma}^k_{\mathbf{m},\mathbf{m}})^{-1}\boldsymbol{\Sigma}^k_{\mathbf{m},\mathbf{R}}, \tag{7}$$

for each given $\mathbf{m}$. The assumption that both petrophysical and elastic variables are distributed as a Gaussian mixture is compatible with the hypothesis of GM distribution for the prior model and it is reasonable if the rock-physics model is not too far from linearity.

However, if these assumptions are not in agreement with well-log data, a nonparametric approach for the conditional probability estimation $P(\mathbf{R}|\mathbf{m})$ should be adopted. In this case, we propose to estimate the joint distribution $P(\mathbf{m},\mathbf{R})$ by applying kernel density estimation on the Monte Carlo samples in a multidimensional domain. Kernel density estimation is a nonparametric technique that allows us to estimate the probability distribution by fitting a base function (the kernel function) at each data point including only those observations close to it.

The joint probability can be expressed as the sum of the contributions of the same kernel function centered at each data-point location (see Silverman, 1986). For example in 2D, if $\mathbf{m} = [I_P]$ and $\mathbf{R} = [\phi]$, then

$$P(\mathbf{m},\mathbf{R}) = P(I_P,\phi) = \frac{1}{N_s h_P h_\phi}\sum_{i=1}^{N_s} K\left(\frac{I_P - I_P^i}{h_P}\right)K\left(\frac{\phi - \phi^i}{h_\phi}\right), \tag{8}$$

where K is the kernel function, $\{I_P^i,\phi^i\}_{i=1,\ldots,N_s}$ are the data samples, and h_P and h_ϕ are the scaling lengths (also called kernel widths). Kernel function K is a nonnegative symmetric function. In this work, we used the Epanechnikov kernel (Doyen, 2007):

$$K(x) = \begin{cases} \frac{3}{4}(1 - x^2) & x \in [-1,1] \\ 0 & \text{otherwise}. \end{cases} \tag{9}$$

For each variable, the scaling lengths control the distance of the observations from the data points and they have to be assessed using training data.

In the current workflow, we estimate the joint distribution by KDE on a multidimensional grid. Then, conditional distribution $P(\mathbf{R}|\mathbf{m})$ can be numerically evaluated by definition

$$P(\mathbf{R}|\mathbf{m}) = \frac{P(\mathbf{m},\mathbf{R})}{\int P(\mathbf{m},\mathbf{R})d\mathbf{R}}, \tag{10}$$

which corresponds to a normalization of the joint probability $P(\mathbf{m},\mathbf{R})$ for each given $\mathbf{m}$.

Probabilistic upscaling

The described method does not explicitly consider the difference in scale and domain of the available data due to different sources of information. In fact, the typical domain of a rock-physics model is depth with the resolution of well logs, whereas inverted seismic attributes are obtained in the time domain with a lower resolution. The objective of this section is to define a step in the methodology that accounts for these differences and is consistent with the general probabilistic approach we are proposing. In general, there are two main is-

sues to take into account in scale-reconciling problems: computation of physically equivalent measures at different scales and correct propagation of the uncertainty from one scale to another.

Upscaling of petrophysical and elastic properties is complicated by the presence of spatial and vertical correlation in the heterogeneities distributions (see, for example, Lake and Srinivasan, 2004). However, in agreement with the choice of our petrophysical inversion model, we concentrate on the problems of coherently transforming different measures from one resolution to another and estimating the corresponding changes in probability distribution. We adopted Backus averaging (Backus, 1962) to face the first problem for elastic properties, and we tackled the second issue by estimating the conditional distribution of elastic parameters at high-resolution scale (fine scale) given the corresponding data at low-resolution scale (coarse scale).

The starting point for the probabilistic scale change is the rock-physics model with the associated uncertainty defined as in equation 1. If $\mathbf{m}^f$ represents the fine-scale (log-scale) vector of the elastic parameters and $\mathbf{m}^c$ the corresponding coarse-scale (seismic) data, we indicate the change of scale with $\mathbf{m}^c = \mathbf{g}(\mathbf{m}^f)$, where function $\mathbf{g}$ represents Backus averaging for velocities and linear average for density.

To integrate the upscaling problem in our probabilistic framework, we propose the following scheme. If $\mathbf{m}^f$ is conditionally distributed with probability $P(\mathbf{m}^f|\mathbf{R})$, the problem of the estimation of the distribution conditioned by $\mathbf{m}^c$ can be solved by generating a set of N_s samples $\{\mathbf{m}_i^f\}_{i=1,\ldots,N_s}$ according to $P(\mathbf{m}^f|\mathbf{R})$ by Monte Carlo simulation, and applying the upscaling transformation $\mathbf{g}$, so we obtain a set of joint samples $\{(\mathbf{m}_i^f,\mathbf{m}_i^c)\}_{i=1,\ldots,N_s}$ that can be used to estimate (with Gaussian models, for example) the conditional distribution $P(\mathbf{m}^f|\mathbf{m}^c)$.

The conditional distribution of the petrophysical parameters given coarse-scale elastic data $P(\mathbf{R}|\mathbf{m}^c)$ can be obtained combining $P(\mathbf{R}|\mathbf{m}^f)$ with $P(\mathbf{m}^f|\mathbf{m}^c)$ by means of the Chapman-Kolmogorov equation (Papoulis, 1984)

$$P(\mathbf{R}|\mathbf{m}^c) = \int_{\mathcal{R}^n} P(\mathbf{R}|\mathbf{m}^f)P(\mathbf{m}^f|\mathbf{m}^c)d\mathbf{m}^f, \tag{11}$$

where n is the dimension of $\mathbf{m}^f$ ($n = 2$ in the case of I_P and I_S). This expression is the probabilistic model that includes uncertainties due to rock physics ($P(\mathbf{R}|\mathbf{m}^f)$) and upscaling ($P(\mathbf{m}^f|\mathbf{m}^c)$).

From seismic to petrophysics inversion

To obtain the posterior distribution of elastic parameters from seismics, we use a linearized AVO inversion technique in a Bayesian framework. The inversion method adopted here assumes an isotropic and elastic medium and it combines the convolutional model with Aki-Richards linearized approximation of Zoeppritz equations valid for vertical weak contrasts, as in Buland and Omre (2003).

If $\mathbf{S}$ refers to seismic data, the elastic model can be expressed as:

$$\mathbf{S} = \mathbf{G}\ell + \mathbf{e}, \tag{12}$$

where $\mathbf{G}$ is the forward linearized operator including both convolution and weak contrasts Aki-Richards approximation, ℓ is the vector of the logarithms of the whole trace of the elastic parameters, and $\mathbf{e}$ is a Gaussian error term with zero mean and covariance $\boldsymbol{\Sigma}_\mathbf{e}$. We also assume that ℓ is distributed according to a multivariate Gaussian prior $\ell \sim N(\ell;\boldsymbol{\mu}_\ell,\boldsymbol{\Sigma}_\ell)$.

Under these hypotheses, it can be shown (Buland and Omre, 2003) that $P(\ell|\mathbf{S})$ is again Gaussian:

$$P(\ell|\mathbf{S}) = N\left(\ell;\boldsymbol{\mu}_{\ell|\mathbf{S}},\boldsymbol{\Sigma}_{\ell|\mathbf{S}}\right), \tag{13}$$

where

$$\boldsymbol{\mu}_{\ell|\mathbf{S}} = \boldsymbol{\mu}_\ell + \boldsymbol{\Sigma}_{\mathbf{S},\ell}^T\left(\boldsymbol{\Sigma}_\mathbf{S}\right)^{-1}(\mathbf{S} - \boldsymbol{\mu}_\mathbf{S}) \tag{14}$$

and

$$\boldsymbol{\Sigma}_{\ell|\mathbf{S}} = \boldsymbol{\Sigma}_\ell - \boldsymbol{\Sigma}_{\mathbf{S},\ell}^T\left(\boldsymbol{\Sigma}_\mathbf{S}\right)^{-1}\boldsymbol{\Sigma}_{\mathbf{S},\ell}. \tag{15}$$

Here, $\boldsymbol{\mu}_\mathbf{S} = \mathbf{G}\boldsymbol{\mu}_\ell$, $\boldsymbol{\Sigma}_\mathbf{S} = \mathbf{G}\boldsymbol{\Sigma}_\ell\mathbf{G}^T + \boldsymbol{\Sigma}_\mathbf{e}$, and $\boldsymbol{\Sigma}_{\mathbf{S},\ell} = \mathbf{G}\boldsymbol{\Sigma}_\ell$ are the cross-covariance between the vector of parameters ℓ and seismic data $\mathbf{S}$.

When the conditional distribution $P(\ell|\mathbf{S})$ is known, then the log-normal distribution $P(\mathbf{m}^c|\mathbf{S}_z)$ can be derived at each vertical position z (assuming a depth conversion of seismic inversion results). The final step to compute the probability of petrophysical variables conditioned by seismic data $P(\mathbf{R}|\mathbf{S}_z)$ including the upscaling effect (equation 11), can be written as

$$P(\mathbf{R}|\mathbf{S}_z) = \int_{\mathcal{R}^n} P(\mathbf{R}|\mathbf{m}^c)P(\mathbf{m}^c|\mathbf{S}_z)d\mathbf{m}^c. \tag{16}$$

By means of equation 16, we finally obtain the posterior probabilities of the petrophysical properties.

We also can introduce a further step to apply the same methodology in the discrete domain, in classification studies of litho-fluid classes, for example. Formally, we compute the probability

$$P(\pi_z|\mathbf{S}_z) = \int_{\mathcal{R}^n} P(\pi_z|\mathbf{R})P(\mathbf{R}|\mathbf{S}_z)d\mathbf{R}, \tag{17}$$

where π_z is the generic litho-fluid class at vertical position z, n is the dimension of $\mathbf{R}$ ($n = 3$, if $\mathbf{R} = [\phi\ sw\ C]^T$), and $P(\pi_z|\mathbf{R})$ is the rock-physics likelihood function.

To generate different realizations of litho-fluid classes conditioned by seismics, including vertical correlation to model the vertical continuity of litho-fluid classes, we can combine the posterior probability (equation 17) with a Markov-chain prior model (as in Larsen et al., 2006)

$$\begin{aligned} P(\pi_z|\mathbf{S}_z) &= \int_{\mathcal{R}^n} P(\pi_z|\mathbf{R})P(\mathbf{R}|\mathbf{S}_z)d\mathbf{R} \\ &\propto \int_{\mathcal{R}^n} P(\mathbf{R}|\pi_z)P(\pi_z)P(\mathbf{R}|\mathbf{S}_z)d\mathbf{R} \propto \\ &\propto \prod_z P(\pi_z|\pi_{z-1})\int_{\mathcal{R}^n} P(\mathbf{R}|\pi_z)P(\mathbf{R}|\mathbf{S}_z)d\mathbf{R}, \end{aligned} \tag{18}$$

where z indicates depth, and the probability $P(\pi_z|\pi_{z-1})$ can be obtained from the downward Markov-chain transition matrix of litho-fluid classes estimated on actual well-log classification (with the assumption that $P(\pi_{z_1}) = P(\pi_{z_1}|\pi_{z_0})$ for notational convenience).

REAL-CASE APPLICATION

Methodology implementation

The methodology application is described for an oil-saturated clastic reservoir, but it can be adapted to different saturation and lithology reservoir conditions, with the choice of a suitable rock-physics model.

First, a rock-physics model is calibrated at well locations using velocity logs and petrophysical curves obtained in formation evaluation analysis. The rock-physics model can be written as

$$[V_P, V_S, \rho] = \mathbf{f}_{RPM}(\phi, sw, C) + \boldsymbol{\varepsilon}, \tag{19}$$

where V_P and V_S are, respectively, P- and S-waves velocities, ρ is the density, ϕ is the effective porosity, sw is the water saturation, C is the clay content, and $\boldsymbol{\varepsilon}$ is the error that represents the difference between model predictions and real data. Function $\mathbf{f}_{RPM}$ can be an empirical relation or a theoretical set of equations such as granular media models or effective media models (see Mavko et al., 2003).

Second, we estimate elastic attributes from seismic data. We use a reformulation of the approximation of Zoeppritz equations by Aki and Richards (1980) in terms of impedances, and we jointly estimate P- and S-impedances and density following the Bayesian approach presented in Buland and Omre (2003). In terms of impedances, the reflection coefficient R_{PP} as a function of the reflection angle θ becomes:

$$R_{PP}(\theta) \sim \frac{1}{2\cos^2\theta}\frac{\Delta I_P}{\bar{I}_P} - 4\frac{\bar{I}_S^2}{\bar{I}_P^2}\sin^2\theta\frac{\Delta I_S}{\bar{I}_S} + \left(\frac{1}{2} - \frac{1}{2\cos^2\theta} + 2\frac{\bar{I}_S^2}{\bar{I}_P^2}\sin^2\theta\right)\frac{\Delta\rho}{\bar{\rho}} \tag{20}$$

where $\bar{I}_P$, $\bar{I}_S$, and $\bar{\rho}$ are, respectively, the averages of impedances and density over the reflecting interface, and ΔI_P, ΔI_S, and $\Delta\rho$ are the corresponding contrasts. With realistic noise levels, the inversion cannot retrieve reliable information about density (as in Buland and Omre, 2003). For this reason, in our real case application we do not use density in the petrophysical inversion workflow.

Finally, we calculate the conditional probabilities of petrophysical variables and litho-fluid classes conditioned by seismics following the methodology described in the theory section:

1) We assume a prior distribution of the petrophysical variables. In our case $P(\phi, sw, C)$ is assumed as a trivariate GMM to account for observed correlations between variables in each litho-fluid class (in this case, the prior is the same at any vertical position).
2) We generate pseudologs of petrophysical properties from the prior distribution with a realistic vertical correlation, in two steps. First, we create profiles of litho-fluid classes, for example, using a first-order Markov-chain downward model (Larsen et al., 2006). Then, in each litho-fluid class, we generate petrophysical properties vertically correlated using a variogram estimated on well data.
3) We apply the rock-physics model $\mathbf{f}_{RPM}$ to the petrophysical pseudologs to obtain the corresponding elastic attributes and we add a random error $\boldsymbol{\varepsilon}$ (equation 19). Then, we compute fine-scale impedances.
4) Using the random samples generated in steps 2 and 3, we estimate the joint probability $P(I_P^f, I_S^f, \phi, sw, C)$, and we derive the conditional probability of petrophysical properties conditioned by impedances $P(\phi, sw, C | I_P^f, I_S^f)$ at fine scale.
5) We upscale the elastic properties applying sequential Backus averaging on a running window, whose length is found by estimating the wavelength from the seismic bandwidth and the average velocity. Then, we compute the conditional probabilities at coarse scale:

$$P(\phi, sw, C | I_P^c, I_S^c) = \int_{\mathcal{R}^2} P(\phi, sw, C | I_P^f, I_S^f) \times P(I_P^f, I_S^f | I_P^c, I_S^c) dI_P^f dI_S^f. \tag{21}$$

6) This last conditional probability is then combined by means of the Chapman-Kolmogorov equation (Papoulis, 1984) with the probability of elastic properties coming from linearized Bayesian inversion $P(I_P^c, I_S^c | \mathbf{S}_z)$, to obtain the posterior probability of petrophysical properties:

$$P(\phi, sw, C | \mathbf{S}_z) = \int_{\mathcal{R}^2} P(\phi, sw, C | I_P^c, I_S^c) P(I_P^c, I_S^c | \mathbf{S}_z) dI_P^c dI_S^c, \tag{22}$$

at each vertical position z.
7) Finally, we estimate the probability of litho-fluid classes conditioned by seismics as

$$P(\pi_z | \mathbf{S}_z) = \int_{\mathcal{R}^3} P(\pi_z | \phi, sw, C) P(\phi, sw, C | \mathbf{S}_z) d\phi ds w dC, \tag{23}$$

and we integrate it with a Markov-chain model by means of equation 18.

In the case of Gaussian mixture assumption, the joint distribution $P(I_P^f, I_S^f, \phi, sw, C)$ is estimated using the EM algorithm (if the rock-physics model were linear, the joint distribution could be analytically derived from the prior). Expectation-maximization is an iterative algorithm that allows us to find maximum likelihood estimates of parameters in probabilistic models in the presence of missing data. It is a two-step method. The expectation step computes an expectation of the log likelihood with respect to the current estimate of the distribution. The maximization step maximizes the expected log likelihood found in the previous step. The algorithm converges to the optimal solution in a number of steps, which depends on different factors such as distribution shape and data dimensions (see Hastie et al., 2002). It is used here to estimate parameters (means and covariance matrices) and weights of Gaussian components of the mixture for joint distribution in the case of multimodality of the data. Once weights and parameters of the joint distribution are known, the conditional distribution is analytically derived using equations 6 and 7.

Alternatively, we propose to use kernel density estimation (KDE), which allows us to estimate a probability density function on a multidimensional grid. In this case, we apply KDE to estimate the joint distribution $P(I_P^f, I_S^f, \phi, sw, C)$, extending equation 8 in a 5D domain. In our implementation, we use the same kernel function (the Epanechnikov kernel) for the five variables and a specific scaling length for each variable. The critical point of this approach is calibration of the scaling lengths: the higher they are, the farther the obser-

vations included in the distribution are from the data points. Choice of scaling lengths depends on the number of data points and the spread of the distribution (Doyen, 2007). Once the joint distribution is estimated, we compute the conditional distribution at fine scale (equation 10) by normalizing the joint distribution at each given (I_P^f, I_S^f).

In both parametric and nonparametric cases, the following steps are similarly performed. A Gaussian model is assumed for the upscaling step and a lognormal distribution is used for seismic inversion. These two probabilities are combined with fine-scale probabilities by means of the Chapman-Kolmogorov equation (equations 21 and 22).

Data application

The methodology has been applied to an oil-saturated clastic reservoir in the North Sea, using angle-stack seismic data and well-log data coming from two wells in the field: well A (relative coordinates: $x = 1530$, $y = 450$) used for model calibration, and well B ($x = 120$, $y = 1000$) used for methodology validation.

Input data for the rock-physics model are the petrophysical curves obtained in formation evaluation analysis: effective porosity, clay content, and water saturation. We focus our attention on a specific reservoir level (Figure 2), where we can identify three litho-fluid classes: oil sand, water sand, and shale. Lithofacies have been obtained by means of log-facies classification, on the basis of the petrophysical curves and the available sedimentologic information. litho-fluid discrimination still remains visible in both the petroelastic and impedances domains (Figure 3).

The adopted rock-physics model is the stiff-sand model (Appendix B) based on Hertz-Mindlin contact theory. The model was previously calibrated on well A (Figure 4) and then used on well B data. For the calibration, we performed a fluid substitution on velocities of well A to obtain corresponding velocities in wet conditions, and we determined the model parameters to obtain a good match with well data. The critical porosity used is 0.4 and the coordination number is 7. Effective pressure in the reservoir is 70 MPa. For the solid phase, we used a matrix model made by two components: sand (mostly made of quartz) and wet clay (mostly made of illite), with the parameters indicated in Table 1. Matrix parameters have been selected on the basis of available mineralogical information about rock composition and for the good match between model predictions and well-log data (Figure 2). The choice of considering clay as a mixture of mineral and clay-bound water is coherent with the choice of using effective porosity.

The stiff-sand model was selected on the basis of available geologic information and because it is appropriate to describe a well-consolidated sand. In shale, the effective porosity is near zero, so the rock-physics model reduces to the computation of velocities and density of a matrix made of wet clay, by means of a Voigt-Reuss-Hill average, and we obtain a good approximation of the velocities in shale.

We describe here implementation of the inversion methodology and its application to the data (we recall that $\mathbf{R} = [\phi \; sw \; C]^T$ and $\mathbf{m} = [I_P \; I_S]^T$). We assume that prior distribution $P(\mathbf{R})$ is a Gaussian mixture (Figure 5) whose weights are the actual proportions of litho-fluid classes. In particular, we assume a Gaussian mixture distribution with truncations for ϕ and C, and a Gaussian mixture score transformation (extension of the normal score transformation) is applied to water saturation sw. The simulation and inversion are conducted from Gaussian mixture scores. At the end of the simulation, results are back-transformed to recover the actual saturation values. If we assume a large variability within each litho-fluid class (large covariance matrices), we also can generate samples that are not present in well data (Figure 5). The advantage of this assumption is that it allows us to simulate the petroelastic properties of different scenarios.

Then, we generate pseudopetrophysical curves in two steps. We first generate profiles of litho-fluid classes by means of a first-order Markov-chain downward model using two transition matrices $\mathbf{P}_1$ and $\mathbf{P}_2$ honoring well A proportions and transition probabilities, respectively, above and under the oil-water contact (at 2182 m):

$$\mathbf{P}_1 = \begin{pmatrix} 0.95 & 0.03 & 0.02 \\ 0.20 & 0.80 & 0 \\ 0.01 & 0.01 & 0.98 \end{pmatrix} \qquad (24)$$

$$\mathbf{P}_2 = \begin{pmatrix} 0.95 & 0.03 & 0.02 \\ 0.06 & 0.94 & 0 \\ 0 & 0.19 & 0.81 \end{pmatrix}.$$

Rows correspond to shale, water sand, and oil sand at generic depth z, and columns refer to shale, water sand, and oil sand at depth $z - 1$ (the downward transition from water sand to oil sand

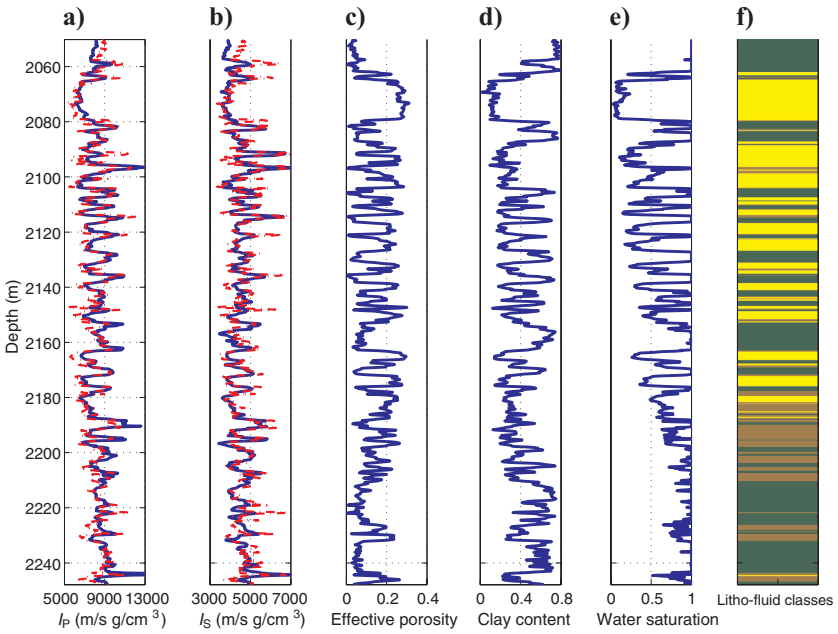

Figure 2. Petrophysical curves derived from log interpretation of well A. From left to right: (a) P-impedance (well log in blue and rock physics model predictions in red), (b) S-impedance (well log in blue and rock-physics model predictions in red), (c) effective porosity, (d) clay content, (e) water saturation, and (f) litho-fluid classification (oil sand in yellow, water sand in brown, shale in green).

is impossible in both cases). If the well information is not representative of reservoir conditions, proportions of litho-fluid classes and, as a consequence, transition matrices can be modified. Then, for each litho-fluid class, we can estimate a variogram to model the vertical correlation of the petrophysical properties (the results for porosity are presented in Figure 6, as an example), and we generate pseudologs of petrophysical properties from the prior with a realistic vertical correlation.

Next, we apply rock-physics model $\mathbf{f}_{\mathrm{RPM}}$ to obtain the corresponding pseudologs of velocities and impedances. Error $\boldsymbol{\varepsilon}$ (see equation 1), added to elastic variables I_{P} and I_{S}, is distributed as a bivariate Gaussian distribution. Its parameters (elements of the covariance matrix) are estimated from the difference between real data and rock-physics model predictions on well A logs ($\sigma_p = 530$ and $\sigma_s = 280$). Using the pseudologs generated by means of the rock-physics model, we perform upscaling using sequential Backus averaging in a running window of about 12.5 m (estimated wavelength is 125 m and operator length is obtained as wavelength/10 as in Avseth et al., 2005), and we estimate the conditional probabilities at coarse scale (equation 21).

Finally, linearized AVO inversion is used to jointly estimate the posterior distribution of P- and S-impedance and density. We estimated the four wavelets independently for each available angle gather. The trend for the prior model was obtained from well logs by filtering impedances logs to a high-cut value of 4 Hz and interpolating these logs along the interpreted horizons. The probabilistic inversion approach is based on the convolutional model and Aki-Richards linearized approximation of Zoeppritz equations in the limit of vertical weak contrasts. Elastic parameters derived from seismic inversion are characterized by a log-Gaussian random field.

Posterior probabilities of petrophysical properties and litho-fluid classes are obtained by means of equations 22 and 23 and the results are shown in the next section.

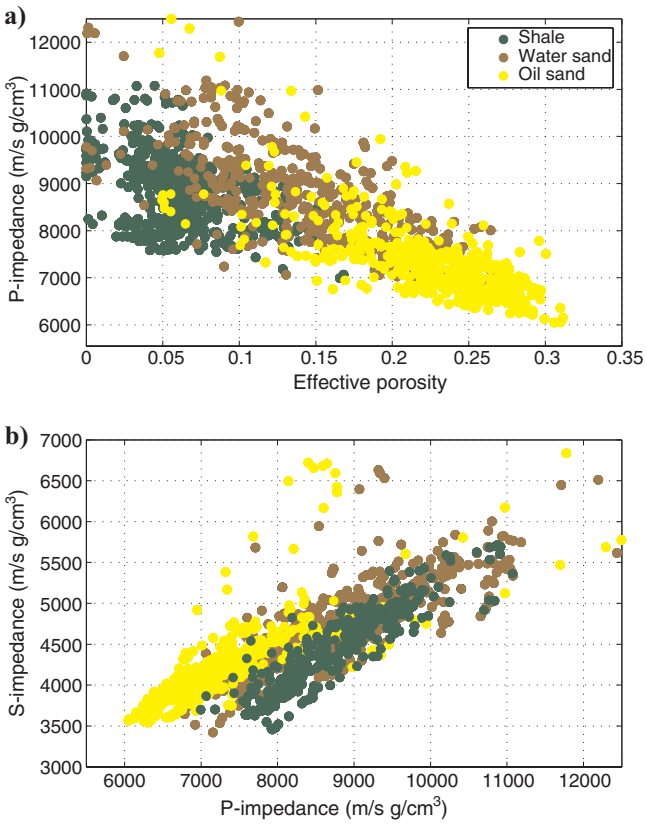

Figure 3. Well-log data distribution and litho-fluid classification of well A. (a) P-impedance versus effective porosity color coded by litho-fluid class. (b) S-impedance versus P-impedance, color-coded by litho-fluid class (oil sand in yellow, water sand in brown, shale in green).

RESULTS

First, we applied the methodology using well-log data from well A and a synthetic seismic trace to verify applicability and validity of the method. Through this feasibility step, we compare two statistical approaches and demonstrate coherent propagation of the uncertainty through the three steps of the method.

Following the approach presented in the previous sections, we will show the results of the petrophysical-properties estimation in three different conditions: at fine scale, at coarse scale, and conditioned by seismic data. In the first step, we take into account only the uncertainty related to the rock-physics model at fine scale, without considering uncertainty associated with coarse scale and with seismics. To estimate the conditional distribution $P(\mathbf{R}|\mathbf{m}^{\mathrm{f}})$, the EM algorithm was applied, assuming three mixture components (one component for each litho-fluid class) combined with the analytical expression of Gaussian mixtures. Figure 7a displays the marginal conditional probabilities of effective porosity, clay content, and water

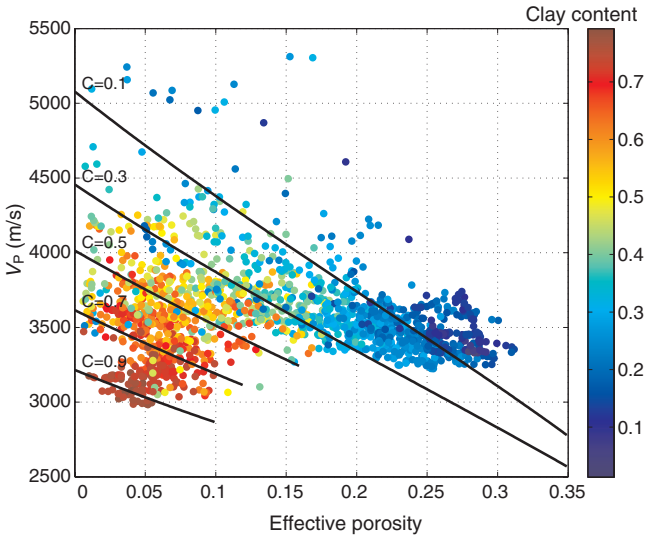

Figure 4. Rock-physics model calibration on well A: velocity in wet condition (obtained performing a fluid substitution on well-log velocities) versus effective porosity, color-coded by clay content. The curves are from the stiff-sand model for a mixture of wet clay and sand, with clay content equal to (from bottom to top) 0.9, 0.7, 0.5, 0.3, and 0.1.

Table 1. Rock-physics model parameters: density ρ, bulk modulus K, and shear modulus μ of the matrix components.

	ρ (g/cm^3)	K (GPa)	μ (GPa)
wet clay	2.5	20	8
sand	2.7	33	36

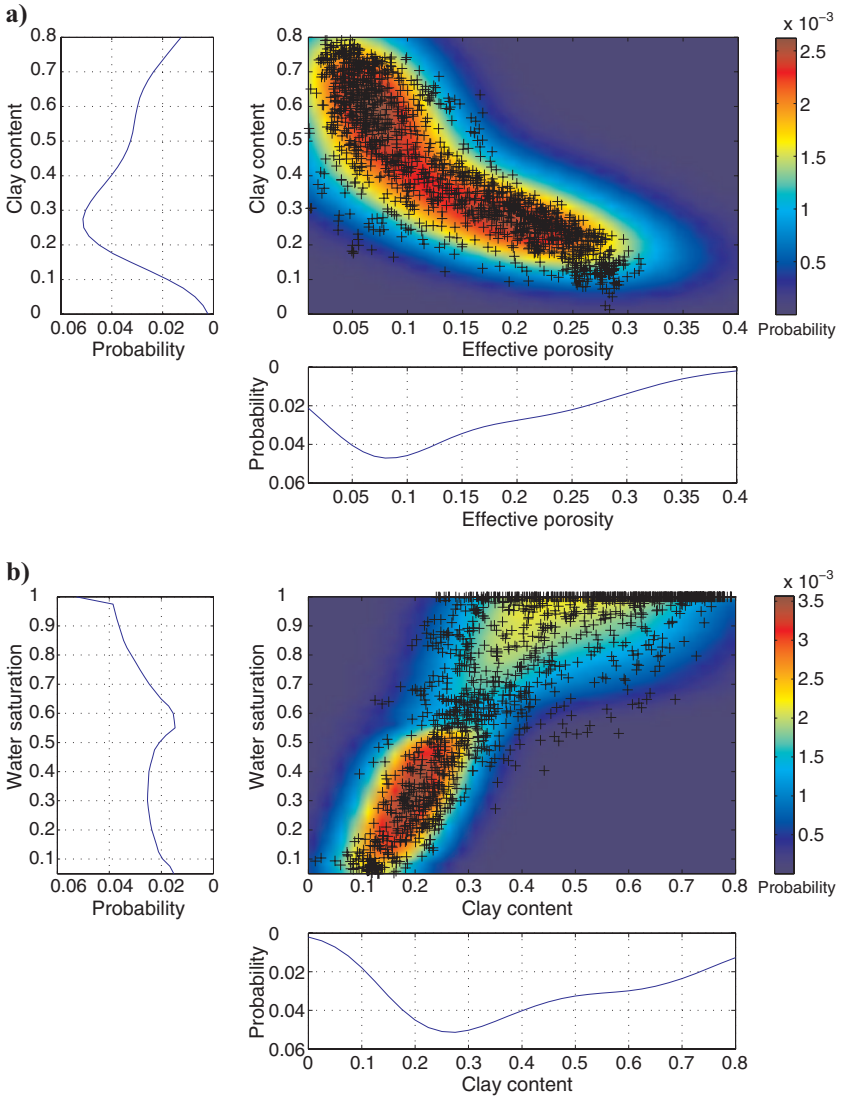

Figure 5. Prior distribution of petrophysical variables. (a) Two-dimensional marginal distribution of effective porosity and clay content with associated 1D marginal distributions. (b) Two-dimensional marginal distribution of clay content and water saturation with associated 1D marginal distributions. Black crosses represent petrophysical data of well A; background color is the joint probability.

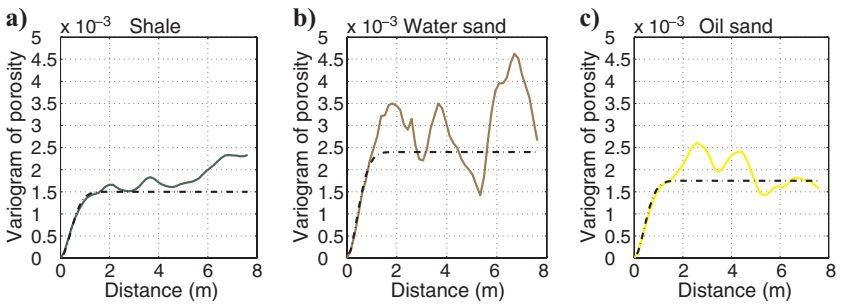

Figure 6. Experimental and fitted variograms of effective porosity for the three litho-fluid classes: variograms of effective porosity in (a) shale, (b) water sand, and (c) oil sand (color lines are the experimental variograms and dotted lines are the fitted variograms).

saturation extracted from $P(\mathbf{R}|\mathbf{m}^{f})$ at fine scale. Because the rock-physics model is accurate, the uncertainty propagated to petrophysics is quite small and the petrophysical-properties estimation honors the actual curves of effective porosity, clay content, and water saturation derived from log interpretation.

Figure 7b shows results of the probability estimation (equation 21) conditioned by upscaled impedances obtained by applying sequential Backus averaging to rock-physics model predictions: the probabilistic upscaling step allows us to take into account the uncertainty associated with the scale change. Comparison between Figure 7a and b clarifies the impact of coarse resolution on uncertainty, which is, as expected, larger in the second case $P(\mathbf{R}|\mathbf{m}^{c})$, especially for water saturation.

Finally, we combined the results of the statistical rock-physics model with seismic inversion performed with the Bayesian approach, by means of equation 22, to obtain an estimation of petrophysical properties conditioned by seismic data $P(\mathbf{R}|\mathbf{S}_z)$. As a feasibility step, we applied the methodology using synthetic seismic data with a signal-to-noise ratio (S/N) equal to 5. Conditional distributions (Figure 8a) show the multimodality of the petrophysical data and the increase of uncertainty, in particular in sequences of thin layers. In the case of multimodal data, the median is not a good estimator, but we can observe that the probability distributions still capture the bimodality of petrophysical properties.

Now we compare the previous results at seismic scale obtained using Gaussian mixture models with results obtained using the kernel density approach (Figure 8). The two results are quite similar: in both cases, petrophysical inversion can capture the bimodality of each variable. The top of the reservoir is characterized by a thick, high-porosity, oil-sand layer, and it is well detected in both cases. In this application, Gaussian mixtures are an appropriate solution and they provide a good result because the litho-fluid classification of well data (which identifies the components of the mixture) allows a good discrimination of petrophysical and elastic properties. Also, the approach based on KDE provides a good estimation of the posterior probability because kernel density estimation recognizes the multimodality of the data if the scaling lengths are correctly chosen. With respect to the GMM approach, the nonparametric approach is more computationally demanding and it requires tuning of the scaling length parameters.

Even though the linear correlation coefficients cannot be used as a full quantitative measure of the inversion quality in the case of multimodal distributions, we tried to evaluate the quality of the match between the inversion results and real

data by computing the correlation coefficients between estimated petrophysical properties and the actual curves (Table 2). Analysis of the correlation coefficients confirms what we observed from the probability densities, in particular, how the scale change affects the uncertainty.

The method also has been applied in a discrete domain, for litho-fluid classification based on seismic data. From the probability distributions of petrophysical properties, we predicted litho-fluid classes (equation 23) at the location of well A, and we used the resulting posterior probabilities to generate multiple realizations of litho-fluid-class vertical sequences. The rock-physics likelihood $P(\pi_z|\mathbf{R})$ has been estimated using petrophysical curves and litho-fluid classification, assuming a Gaussian distribution for each litho-fluid class.

Results of the classification conditioned by seismic are shown in Figure 9a: we can observe a high probability value for the oil-sand class, reflecting the thick, high-porosity sand layer at the top of the reservoir. It is important to observe that, even though the maximum a posteriori (MAP) of probabilities of litho-fluid classes is not a good estimator in this case, fluctuations of the probability curves have a good match with the actual profile of litho-fluid classes and they can be used as a prior probability for multiple realizations. Integrating the probability of litho-fluid classes conditioned by seismics with probability obtained from transition matrices (equation 18), we can generate several realizations of litho-fluid-class profiles at well location A (Figure 9b).

We used contingency analysis (Table 3) to evaluate misclassification errors, comparing the maximum a posteriori of the probability $P(\pi_z|\mathbf{S}_z)$ with the actual classification. In the contingency table, we computed the absolute frequencies, reconstruction rate, recognition rate, and estimation index. The reconstruction rate is obtained by normalizing the frequency table per row, and the recognition rate is obtained by normalizing the frequency table per column. The reconstruction rate represents the percentage of samples belonging to a litho-fluid class (actual), which are classified in that class (predicted). The recognition rate represents the percentage of samples classified in a litho-fluid class (predicted) that actually belong to that class (actual). Information concerning under/overestimation can be inferred from the estimation index, which is defined as the difference between the reconstruction rate and recognition rate. A negative estimation index in the main diagonal indicates underestimation, and a positive estimation index indicates overestimation; the off-diagonal terms describe in which class the samples are misclassified. In our case, oil sand could be reconstructed by 70.5% by the inversion algorithm and recognized by 62.5%, thus, sand is overestimated (estimation index 8%). The actual oil-sand samples not detected by the inversion are mostly classified in shale (96 samples, reconstruction rate 19.4%). The recognition rates of predicted oil sand tell us that some shale samples (108) and water-sand samples (101) are classified in oil sand, which is the reason for the overestimation of oil sand. Similarly, the negative estimation index for water sand (-7.8%) in the main diagonal of the contingency table shows an underestimation of water sand. In some cases, we cannot discriminate water sand from actual shale and oil sand from actual water sand (relatively high estimation index of predicted water sand in actual shale and of predicted oil sand in actu-

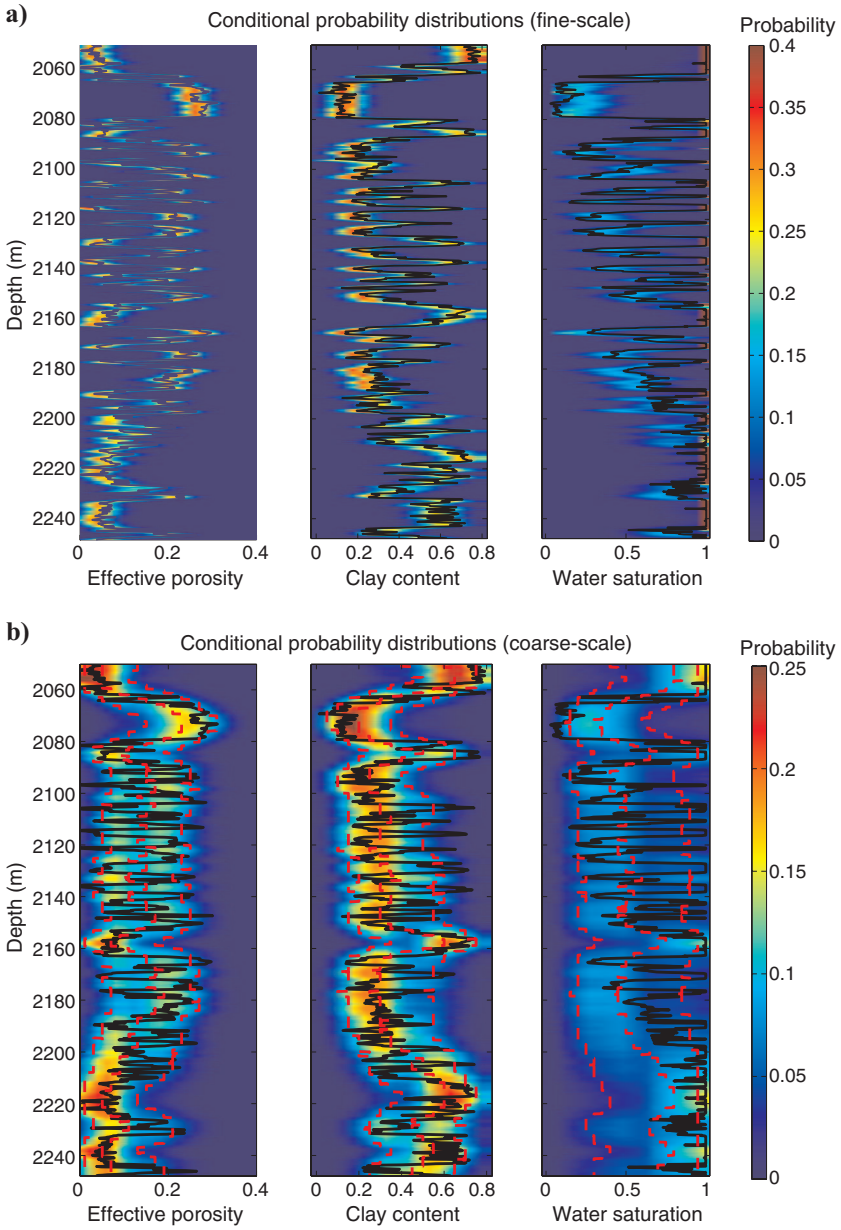

Figure 7. Petrophysical-properties estimation at well A location: effective-porosity, clay-content, and water-saturation probability distributions obtained with GMM. (a) Petrophysical-properties estimation conditioned by high-resolution impedances, extracted from $P(\mathbf{R}|\mathbf{m}^f)$. (b) Petrophysical-properties estimation conditioned by upscaled data, extracted from $P(\mathbf{R}|\mathbf{m}^c)$. The background color is the conditional probability. Black lines are the actual petrophysical curves, red dashed lines represent P10, median, and P90.

al water sand). This result can be justified by the rock-physics template (Figure 3), where we can note the overlaps between those classes. Misclassification between oil sand and shale is due mainly to the upscaling effect on thin layers.

Finally, we applied the methodology to the whole reservoir level using real seismics to obtain 3D volumes of petrophysical properties with the associated uncertainty. First, we performed a Bayesian inversion on a small 3D volume, including well A (used for rock-physics model calibration) and well B (used for methodology validation). The seismic volume (four angle gathers available) contains about 10,000 traces in a time window corresponding to a depth interval of approximately 250 m. In Figure 10, we display two seismic sections (related to the partial angle stacks 20° and 44°), passing through the two wells. In Figure 11, we show the prior model used for inversion and the inverted values with the associated uncertainties at well locations. The corresponding inverted impedances sections I_P and I_S, estimated by Bayesian inversion, are displayed in Figure 12.

The final result of this study is the posterior probability of petrophysical properties on the entire 3D volume. Figure 13 shows the probability distributions of effective porosity at three locations along the 2D section passing through the wells. Comparison between actual effective-porosity curves and estimated probabilities gives evidence that at the top of the reservoir, estimation is more accurate than in the lower part. In Figure 14, we display the maximum a

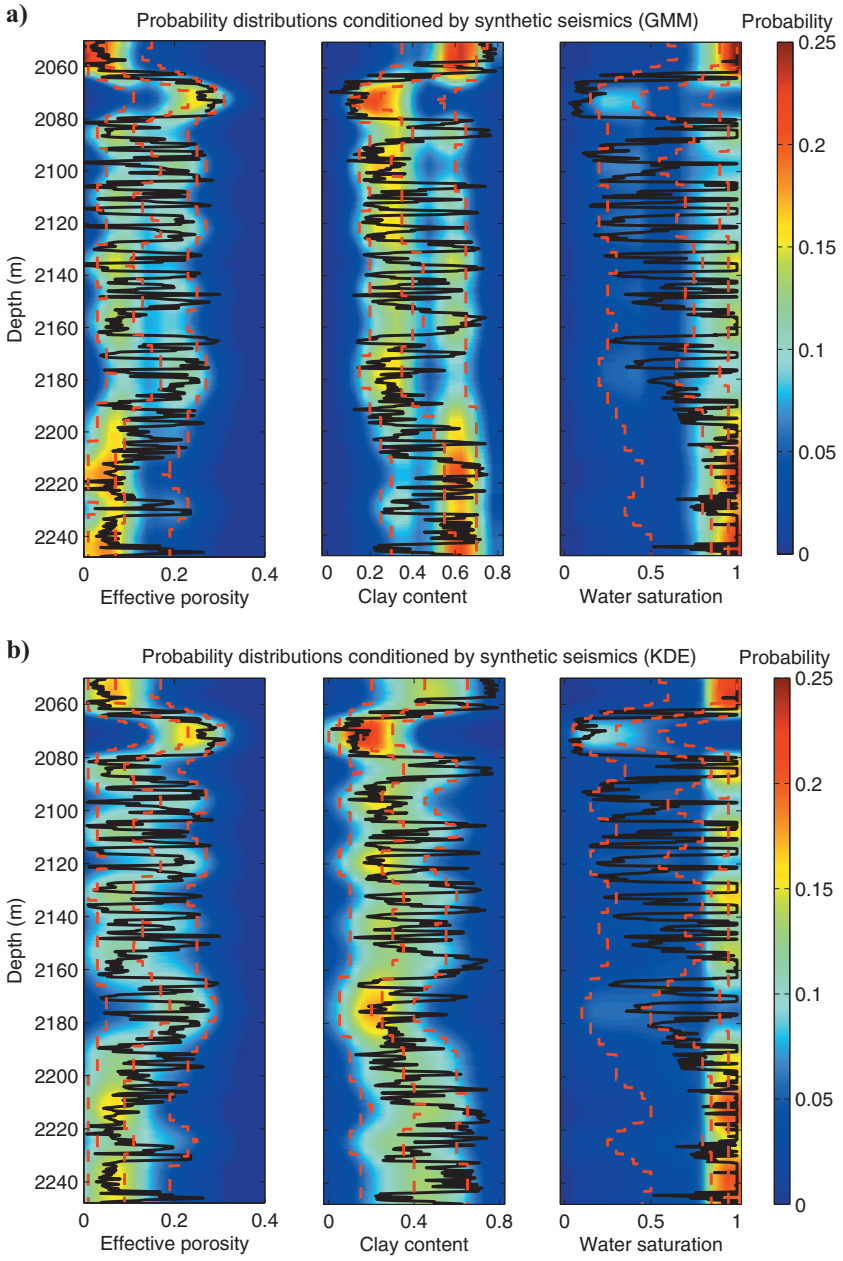

Figure 8. Petrophysical-properties estimation conditioned by synthetic seismic data at well A location: effective-porosity, clay-content, and water-saturation probability distributions extracted from $P(\mathbf{R}|\mathbf{S}_z)$, computed with (a) GMM and (b) KDE. The background color is the conditional probability. Black lines are the actual petrophysical curves, red dashed lines represent P10, median, and P90.

Table 2. Correlation coefficients between estimated petrophysical properties and real data at well A location.

	Correlation coefficient of effective porosity	Correlation coefficient of clay content	Correlation coefficient of water saturation
Conditioned by fine-scale data	0.95	0.89	0.87
Conditioned by coarse-scale data	0.55	0.67	0.63
Conditioned by synthetic seismics (GMM)	0.58	0.55	0.64
Conditioned by synthetic seismics (KDE)	0.55	0.60	0.69

posteriori of the posterior probabilities of effective porosity, clay content, and water saturation. In the upper part of the reservoir, we can clearly detect the overcap clay and the top of the reservoir, characterized by a high-porosity sand filled by oil. In the lower part, thin layers observed in the well logs are not detected and the uncertainty associated with the inverted properties increases. This is mainly due to quality of the seismic data, which is higher at the top (S/N$\simeq$3) and very poor at the bottom (S/N$\simeq$1), as we can observe in the seismic sections (Figure 10).

We also performed a litho-fluid classification based on seismic data. Figure 15 shows the curves of conditional probabilities of litho-fluid classes at the location of well A, conditioned by the corresponding seismic trace and some realizations obtained integrating the posterior probability of

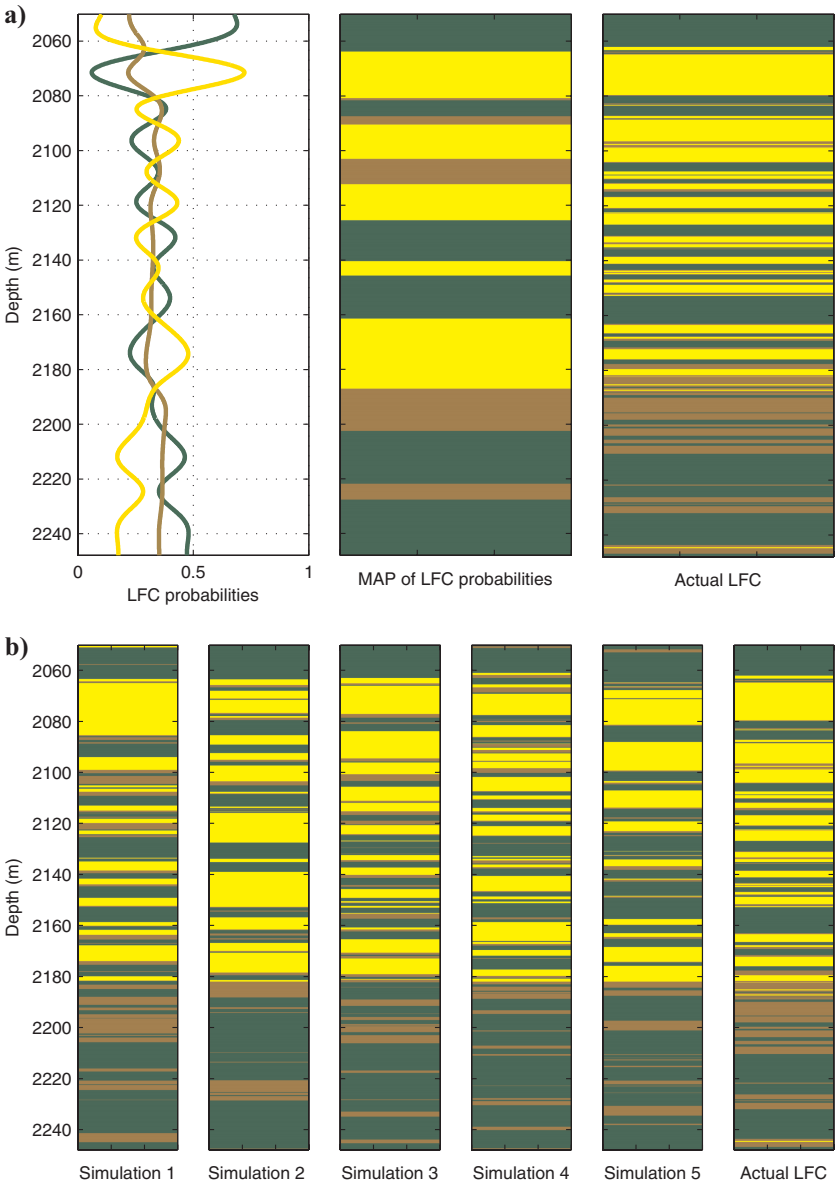

Figure 9. Litho-fluid probabilistic classification conditioned by synthetic seismics at well A location. (a) From left to right: probabilities of litho-fluid classes $P(\pi_z|\mathbf{S}_z)$ based on petrophysical inversion, MAP of the probability and actual litho-fluid classes. (b) Some realizations obtained with a Markov-chain approach (oil sand in yellow, water sand in brown, shale in green).

litho-fluid classes with the Markov-chain model. The quality of Markov-chain realizations is acceptable at the top of the reservoir and quite poor at the bottom, where the S/N of seismic data is very low.

Figure 16 illustrates results for the 3D volume (for example, for effective porosity) by extracting a crossline passing for well B and an inline for well A. Finally, in Figure 17, we propose a 3D visualization of hydrocarbon-sands probability: the oil-sand probability cube has been truncated to reveal areas where the probability of oil-sand litho-fluid-class occurrence is greater than 0.7.

DISCUSSION

The feasibility test based on synthetic seismics shows propagation of different sources of uncertainty through different steps and the applicability of this methodology with both proposed statistical approaches. The real-case application, integrating well data and real seismics, shows that the results are quite satisfactory as long as the quality of the seismics is acceptable. In particular, the use of Gaussian mixtures seems to be a valid approach for classification of petrophysical and categorical parameters, which can be applied to real cases with reduced computational time.

Application of the rock-physics model is not computationally demanding, whereas estimation of the conditional probability in a Bayesian framework can be quite hard to obtain because it requires estimation of the joint distribution in a space of high dimensions. Gaussian mixture models are a suitable solution because of their analytical convenience, especially when the distributions of petrophysical and elastic attributes describe features of different litho-fluid classes. The nonparametric alternative, kernel-density estimation, is more computationally demanding because it requires numerical evaluation of a joint probability on a multidimensional domain. A more efficient method to tackle the multidimensional extension of KDE is based on fast Fourier transform (FFT). In fact, KDE also can be seen as a convolution, so that we can reduce computational time by realizing the convolution by means of FFT (Buland et al., 2008). However, one of the most critical points in estimating probabilities by means of kernel density is the choice of scaling length parameters, which must be determined through different trials.

The main simplification we adopted in our approach is overlooking the spatial correlation of petrophysical variables for the estimation of conditional distributions, to reduce the dimension of the probability space. We do take into account the vertical correlation in seismic inversion by including a vertical correlation in the prior covariance matrix of the vector of elastic parameters and in the prior covariance matrix of the error on seismic amplitudes for each angle gather (Buland and Omre, 2003). However, the spatial correlation is not explicitly accounted for because we adopt a trace-by-trace inversion approach to jointly estimate impedances and densities from seismics. We remark that the lateral continuity of our results is mainly related to the imaging: in fact, part of the lateral correlation of seismic data is imposed by the migration operator which is a spatial filter whose correlation length is associated with the Fresnel zone.

To perform the final step from continuous petrophysical variables to litho-fluid-class modeling, Gaussian mixture models seem to be an appropriate approach as they can express the multimodal features of petrophysical variables in different litho-fluid classes. Integration of more advanced geostatistical techniques could be a significant improvement to use probabilistic information related to litho-fluid classes to generate multiple realizations for reservoir characterization.

Table 3. Contingency analysis of petrophysical-properties estimation at well A location (*f* is absolute frequency, *R* is reconstruction rate, *r* is recognition rate, and *E* is the estimation index).

	Predicted shale	Predicted water sand	Predicted oil sand
Shale			
f	472	104	108
R	69.0%	15.2%	15.8%
r	69.2%	40.0%	19.4%
E	−0.2%	−24.8%	−3.6%
Water sand			
f	114	106	101
R	35.5%	33.0%	31.5%
r	16.7%	40.8%	18.1%
E	18.8%	−7.8%	13.4%
Oil sand			
f	96	50	349
R	19.4%	10.1%	70.5%
r	14.1%	19.2%	62.5%
E	5.3%	−9.1%	8.0%

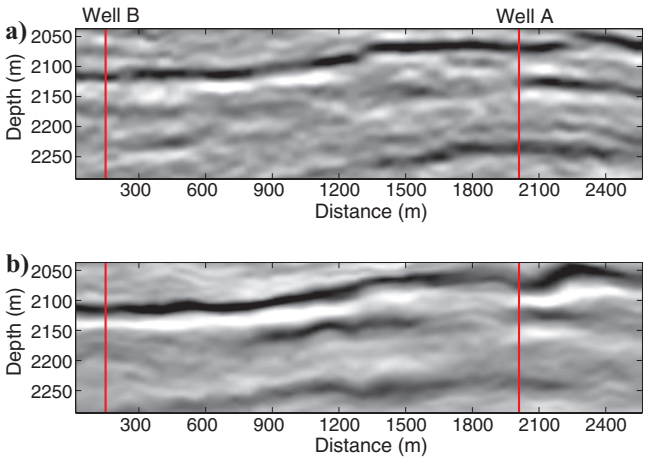

Figure 10. 2D seismic sections passing through well A (on the right) and well B (on the left): (a) angle stack 20°, and (b) angle stack 44°.

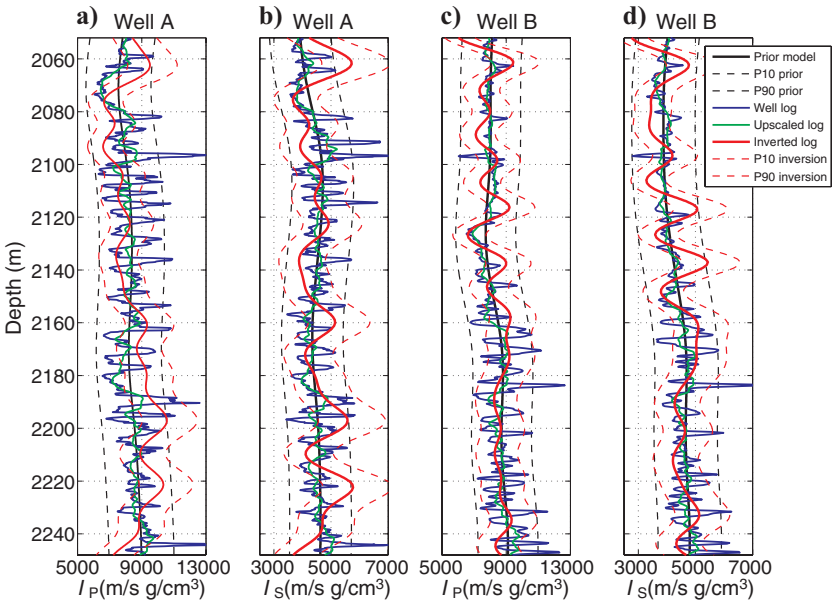

Figure 11. Prior model and posterior distributions at wells locations. (a) P-impedance of well A, (b) S-impedance of well A, (c) P-impedance of well B, and (d) S-impedance of well B. Blue curves are the actual logs, green curves represent the upscaled data, black curves are the prior model, and red curves represent the inverted values. Dashed lines represent P10 and P90.

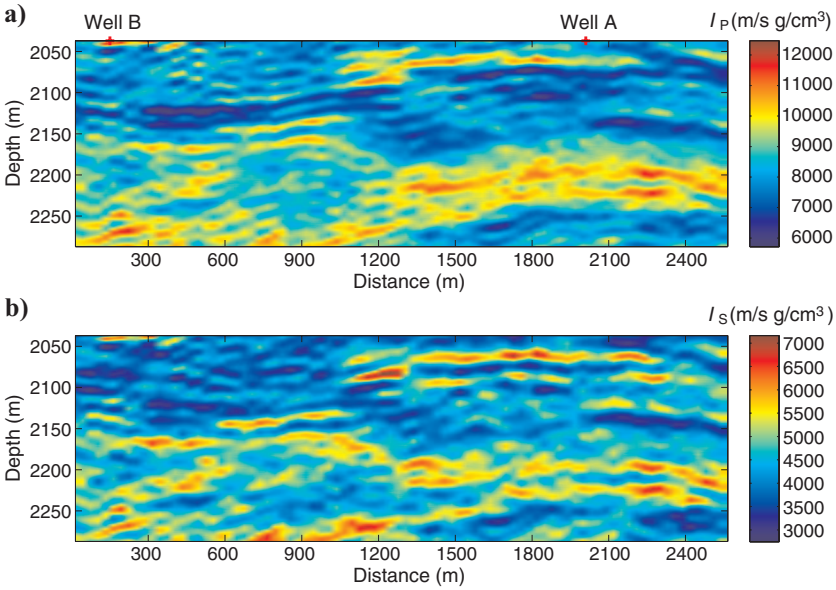

Figure 12. Two-dimensional sections of inverted impedances: (a) inverted P-impedance, (b) inverted S-impedance.

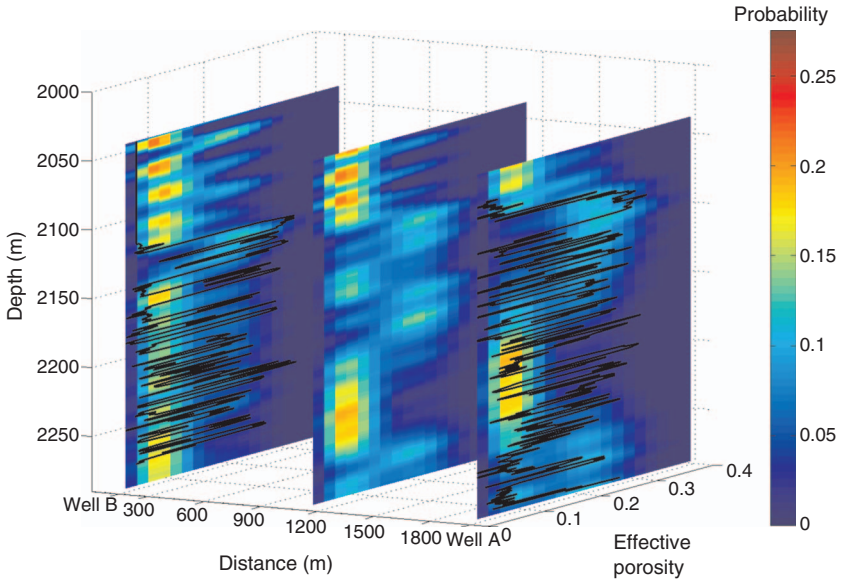

Figure 13. Probability distributions of effective porosity at wells locations (well A on the right, well B on the left) and at an intermediate location between the two wells. Black lines are the actual effective porosity curves.

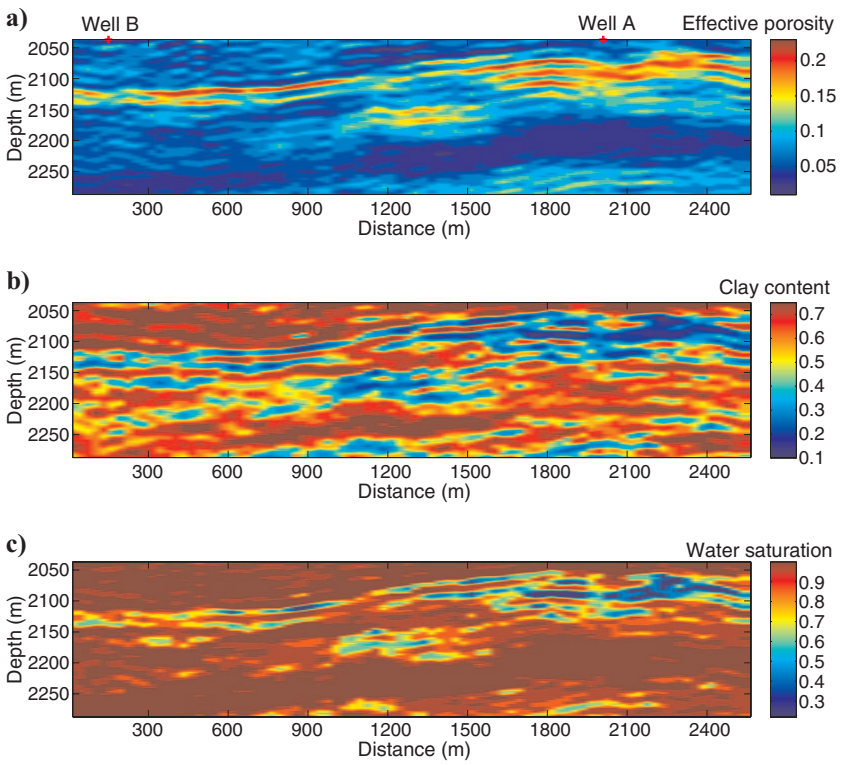

Figure 14. Estimations of (a) effective porosity, (b) clay content, and (c) water saturation in the 2D section obtained from the mode of the posterior distributions.

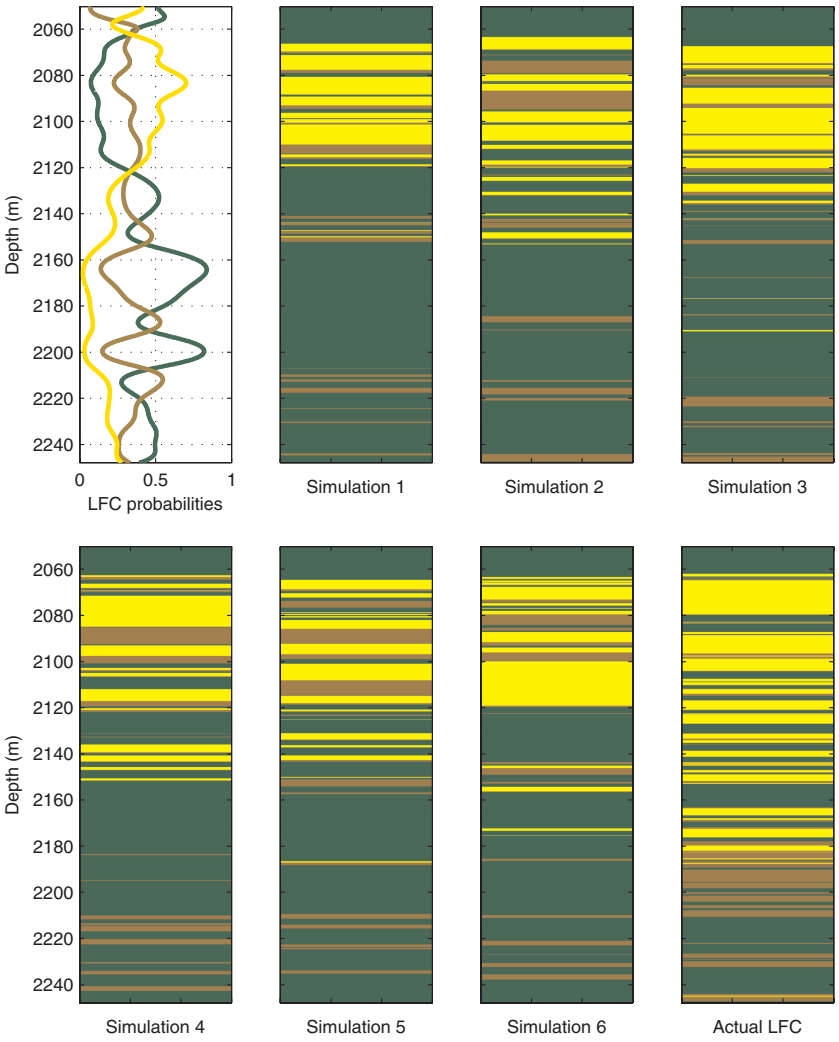

Figure 15. Litho-fluid probabilistic classification conditioned by real seismics at well A location. (a) From left to right: probabilities of litho-fluid classes $P(\pi_z|\mathbf{S}_z)$ based on petrophysical inversion, and three realizations obtained with a Markov-chain approach. (b) From left to right: three more realizations obtained with a Markov-chain approach compared with actual litho-fluid classification (oil sand in yellow, water sand in brown, shale in green).

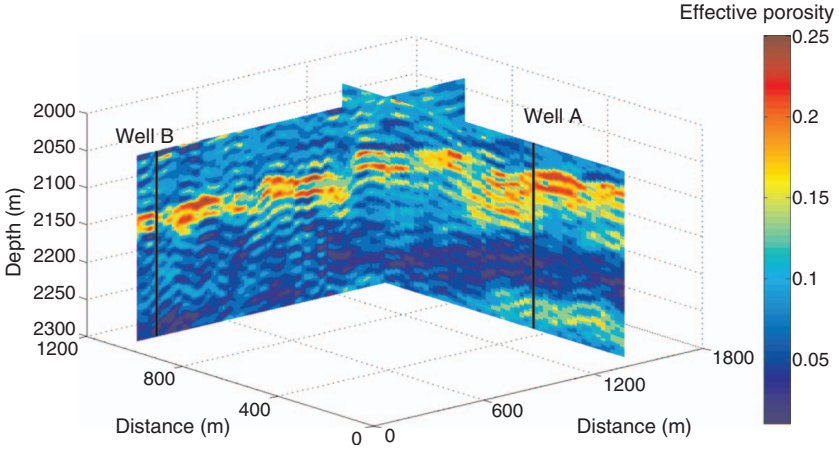

Figure 16. Estimation of effective porosity along two lines extracted from the 3D volume.

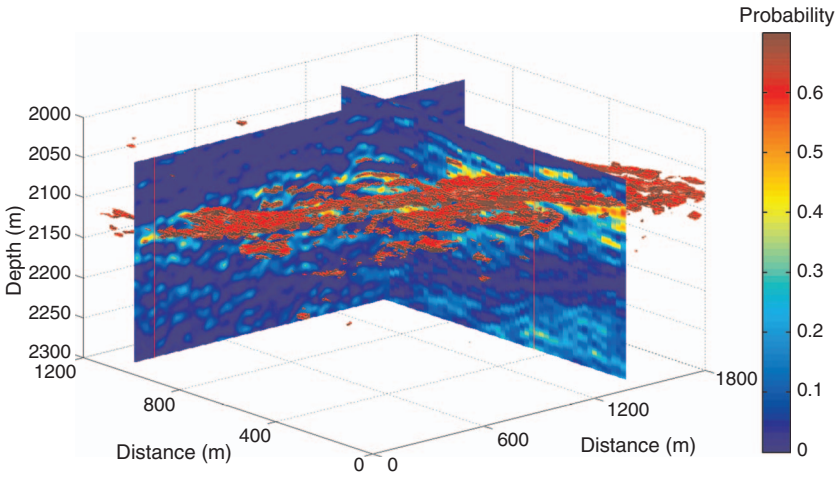

Figure 17. Isoprobability surface of 70% probability of oil-sand litho-fluid class. The background slices represent two 2D sections of probability of oil-sand occurrence.

CONCLUSIONS

The presented methodology aims to propagate the uncertainty from seismic to petrophysical properties, including the effect of scale change, seismic noise error, and the degree of approximation of physical models. Statistical rock physics, combined with the probabilitic approach adopted for seismic inversion, has been proposed to quantify the uncertainty. The main results of the method are the probability distributions of estimated petrophysical parameters, which can be used to assess the reliability of reservoir-properties estimation. To obtain the posterior distribution of petrophysical properties, we note that one key point of our method is the use of Gaussian mixture models and identification of weights of the mixture as the probability of litho-fluid classes.

Even though the considered uncertainty factors do not cover all the possible sources, the 1D feasibility test shows that the main effects due to scale changes and seismic noise are taken into account and that these two factors can explain an important part of the uncertainty.

In the application case, the method works better in the upper layers, where the signal-to-noise ratio is high, rather than in the lower layers, where signal-to-noise is low. In conclusion, where signal-to-noise is acceptable, probabilistic petrophysical evaluation on the real case shows the applicability of the method and that reliability of the seismic data is coherently propagated to petrophysical-properties prediction.

The proposed method can be applied to all reservoirs where elastic characterization of petrophysical properties is possible and where the physical link can be described by a suitable rock-physics model.

ACKNOWLEDGMENTS

We acknowledge Eni e&p management for permission to publish this paper, Eni Norge for data access, Enrico Paparozzi (Eni e&p) for collaboration, and reviewers for helpful suggestions and comments.

APPENDIX A

PROBABILISTIC FORMULATION

Here we recall analytical results for conditional distributions of Gaussian mixtures, extending results valid in the Gaussian case. If the joint distribution is a Gaussian mixture of N_c components, we indicate the joint probability as

$$P(\mathbf{m},\mathbf{R}) = \sum_{k=1}^{N_c} \pi_k N(\mathbf{y};\boldsymbol{\mu}_{\mathbf{y}}^k,\boldsymbol{\Sigma}_{\mathbf{y}}^k) \quad \text{(A-1)}$$

where $\mathbf{y} = \begin{bmatrix}\mathbf{m}\\ \mathbf{R}\end{bmatrix}$. The mean and covariance of each component are given by

$$\boldsymbol{\mu}_{\mathbf{y}}^k = \begin{bmatrix}\boldsymbol{\mu}_{\mathbf{m}}^k\\ \boldsymbol{\mu}_{\mathbf{R}}^k\end{bmatrix}, \quad \boldsymbol{\Sigma}_{\mathbf{y}}^k = \begin{bmatrix}\boldsymbol{\Sigma}_{\mathbf{m},\mathbf{m}}^k & \boldsymbol{\Sigma}_{\mathbf{m},\mathbf{R}}^k\\ \boldsymbol{\Sigma}_{\mathbf{R},\mathbf{m}}^k & \boldsymbol{\Sigma}_{\mathbf{R},\mathbf{R}}^k\end{bmatrix}. \quad \text{(A-2)}$$

Then conditional distribution $P(\mathbf{R}|\mathbf{m})$ is again a Gaussian mixture (see, for example, Dovera and Della Rossa, 2007):

$$P(\mathbf{R}|\mathbf{m}) = \sum_{k=1}^{N_c} \lambda_k N\left(\mathbf{R};\boldsymbol{\mu}_{\mathbf{R}|\mathbf{m}}^k,\boldsymbol{\Sigma}_{\mathbf{R}|\mathbf{m}}^k\right). \quad \text{(A-3)}$$

Here, λ_k are the weights of the conditional distribution

$$\lambda_k(\mathbf{m}) = \frac{\pi_k N\left(\mathbf{R};\boldsymbol{\mu}_{\mathbf{R}|\mathbf{m}}^k,\boldsymbol{\Sigma}_{\mathbf{R}|\mathbf{m}}^k\right)}{\sum_{\ell=1}^{N_c} \pi_\ell N\left(\mathbf{R};\mu_{\mathbf{R}|\mathbf{m}}^\ell,\boldsymbol{\Sigma}_{\mathbf{R}|\mathbf{m}}^\ell\right)}, \quad \text{(A-4)}$$

and the mean and covariance of each component of the conditional distribution can be analytically derived as

$$\boldsymbol{\mu}_{\mathbf{R}|\mathbf{m}}^k = \boldsymbol{\mu}_{\mathbf{R}}^k + \boldsymbol{\Sigma}_{\mathbf{R},\mathbf{m}}^k (\boldsymbol{\Sigma}_{\mathbf{m},\mathbf{m}}^k)^{-1}(\mathbf{m} - \boldsymbol{\mu}_{\mathbf{m}}^k) \quad \text{(A-5)}$$

and

$$\boldsymbol{\Sigma}_{\mathbf{R}|\mathbf{m}}^k = \boldsymbol{\Sigma}_{\mathbf{R},\mathbf{R}}^k - \boldsymbol{\Sigma}_{\mathbf{R},\mathbf{m}}^k (\boldsymbol{\Sigma}_{\mathbf{m},\mathbf{m}}^k)^{-1}\boldsymbol{\Sigma}_{\mathbf{m},\mathbf{R}}^k \quad \text{(A-6)}$$

for each given $\mathbf{m}$.

APPENDIX B

ROCK-PHYSICS MODEL

The stiff-sand model is based on Hertz-Mindlin grain-contact theory (see Mavko et al., 2003). This model provides estimations for bulk K_{HM} and shear μ_{HM} moduli of a dry rock, assuming that the sand frame is a dense random pack of identical spherical grains subject to an effective pressure P with a given porosity ϕ_0 and an average number of contacts per grain n (coordination number):

$$K_{HM} = \sqrt[3]{\frac{n^2(1-\phi_0)^2\mu_{mat}^2 P}{18\pi^2(1-\nu)^2}} \quad \text{(B-1)}$$

and

$$\mu_{HM} = \frac{5-4\nu}{10-5\nu}\sqrt[3]{\frac{3n^2(1-\phi_0)^2\mu_{mat}^2 P}{2\pi^2(1-\nu)^2}}, \quad \text{(B-2)}$$

where ν is the grain Poisson's ratio and μ_{mat} is the matrix shear modulus.

Matrix elastic moduli are obtained by Voigt-Reuss-Hill averages for a matrix made of two components, wet clay (mixture of clay and clay-bound water) and sand:

$$K_{mat} = \frac{1}{2}\left(\frac{CK_c + (1-C)K_s}{1-\phi} + \frac{1-\phi}{\frac{C}{K_c} + \frac{1-C}{K_s}}\right) \quad \text{(B-3)}$$

and

$$\mu_{mat} = \frac{1}{2}\left(\frac{C\mu_c + (1-C)\mu_s}{1-\phi} + \frac{1-\phi}{\frac{C}{\mu_c} + \frac{1-C}{\mu_s}}\right), \quad \text{(B-4)}$$

where C is the volume of wet clay, ϕ is the effective porosity, and K_c, μ_c, K_s, and μ_s, are, respectively, the bulk and shear moduli of wet clay and sand.

For effective porosity values between zero and the critical porosity ϕ_0, this model connects the solid-phase elastic moduli K_{mat} and μ_{mat} respectively, with the elastic moduli K_{HM} and μ_{HM} of the dry rock at porosity ϕ_0, by interpolating these two end members at the intermediate effective-porosity values by means of the modified Hashin-Shtrikman upper bound:

$$K_{dry} = \left[\frac{\phi/\phi_0}{K_{HM} + \frac{4}{3}\mu_{mat}} - \frac{1-\phi/\phi_0}{K_{mat} + \frac{4}{3}\mu_{mat}}\right]^{-1} - \frac{4}{3}\mu_{mat}, \quad \text{(B-5)}$$

$$\mu_{dry} = \left[\frac{\phi/\phi_0}{\mu_{HM} + \frac{1}{6}\xi\mu_{mat}} - \frac{1-\phi/\phi_0}{\mu_{mat} + \frac{1}{6}\xi\mu_{mat}}\right]^{-1} - \frac{1}{6}\xi\mu_{mat}, \quad \text{(B-6)}$$

where

$$\xi = \frac{9K_{mat} + 8\mu_{mat}}{K_{mat} + 2\mu_{mat}}.$$

Gassmann's equations are used for calculating the effect of fluid on velocities using matrix and fluid properties (see Dvorkin et al., 2007 for the use of effective porosity in Gassmann):

$$K_{sat} = K_{dry} + \frac{\left(1 - \frac{K_{dry}}{K_{mat}}\right)^2}{\frac{\phi}{K_{fl}} + \frac{1-\phi}{K_{mat}} - \frac{K_{dry}}{K_{mat}^2}} \quad \text{(B-7)}$$

and

$$\mu_{sat} = \mu_{dry}. \quad \text{(B-8)}$$

From the saturated-rock elastic moduli, we finally obtain velocities as

$$V_P = \sqrt{\frac{K_{sat} + \frac{4}{3}\mu_{sat}}{\rho}} \quad \text{(B-9)}$$

and

$$V_S = \sqrt{\frac{\mu_{sat}}{\rho}}, \quad \text{(B-10)}$$

where ρ is the density of the saturated rock, estimated as a weighted linear average.

REFERENCES

Aki, K., and P. G. Richards, 1980, Quantitative seismology: W. H. Freeman & Co.

Avseth, P., T. Mukerji, and G. Mavko, 2005, Quantitative seismic interpretation: Cambridge University Press.

Bachrach, R., 2006, Joint estimation of porosity and saturation using stochastic rock-physics modeling: Geophysics, **71**, no. 5, O53–O63.

Backus, G. E., 1962, Long-wave elastic anisotropy produced by horizontal layering: Journal of Geophysical Research, **67**, 4427–4440.

Bosch, M., C. Carvajal, J. Rodrigues, A. Torres, M. Aldana, and J. Sierra, 2009, Petrophysical seismic inversion conditioned to well-log data: Methods and application to a gas reservoir: Geophysics, **74**, no. 2, O1–O15.

Buland, A., O. Kolbjørnsen, R. Hauge, O. Skjæveland, and K. Duffaut, 2008, Bayesian lithology and fluid prediction from seismic prestack data: Geophysics, **73**, no. 3, C13–C21.

Buland, A., and H. Omre, 2003, Bayesian linearized AVO inversion: Geophysics, **68**, 185–198.

Dovera, L., and E. Della Rossa, 2007, Ensemble Kalman filter for Gaussian mixture models: Petroleum Geostatistics 2007, EAGE, Proceedings, A16.

Doyen, P., 2007, Seismic reservoir characterization: EAGE.

Dvorkin, J., G. Mavko, and B. Gurevich, 2007, Fluid substitution in shaley sediment using effective porosity: Geophysics, **72**, no. 3, O1–O8.

Eidsvik, J., P. Avseth, H. Omre, T. Mukerji, and G. Mavko, 2004, Stochastic reservoir characterization using prestack seismic data: Geophysics, **69**, 978–993.

Gallop, J., 2006, Facies probability from mixture distributions with non-stationary impedance errors: 76th Annual International Meeting, SEG, Expanded Abstracts, 1801–1805.

González, E. F., T. Mukerji, and G. Mavko, 2008, Seismic inversion combining rock physics and multiple-point geostatistics: Geophysics, **73**, no. 1, R11–R21.

Gunning, J., and M. Glinsky, 2007, Detection of reservoir quality using Bayesian seismic inversion: Geophysics, **72**, no. 3, R37–R49.

Hastie, T., R. Tibshirani, and J. Friedman, 2002, The elements of statistical learning: Springer.

Lake, L. W., and S. Srinivasan, 2004, Statistical scale-up of reservoir properties: Concepts and applications: Journal of Petroleum Science & Engineering, **44**, 27–39.

Larsen, A. L., M. Ulvmoen, H. Omre, and A. Buland, 2006, Bayesian lithology/fluid prediction and simulation on the basis of a Markov-chain prior model: Geophysics, **71**, no. 5, R69–R78.

Mavko, G., T. Mukerji, and J. Dvorkin, 2003, The rock physics handbook: Cambridge University Press.

Mukerji, T., A. Jørstad, P. Avseth, G. Mavko, and J. R. Granli, 2001, Mapping lithofacies and pore-fluid probabilities in a North Sea reservoir: Seismic inversions and statistical rock physics: Geophysics, **66**, 988–1001.

Papoulis, A., 1984, Probability, random variables and stochastic processes: McGraw-Hill.

Sengupta, M., and R. Bachrach, 2007, Uncertainty in seismic-based pay volume estimation: Analysis using rock physics and Bayesian statistics: The Leading Edge, **24**, 184–189.

Silverman, B. W., 1986, Density estimation for statistics and data analysis monographs on statistics and applied probability: Chapman & Hall.

Spikes, K., T. Mukerji, J. Dvorkin, and G. Mavko, 2008, Probabilistic seismic inversion based on rock-physics models: Geophysics, **72**, no. 5, R87–R97.

Tarantola, A., 2005, Inverse problem theory: SIAM.